Mass-metallicity relation from z=5 to the present: Evidence for a transition in the mode of galaxy growth at z=2.6 due to the end of sustained primordial gas infall

P. Møller,[1]⋆ J. P. U. Fynbo,[2] C. Ledoux,[3] K. K. Nilsson,[1]

[1]*European Southern Observatory, Karl-Schwarzschildstrasse 2, 85748 Garching bei München, Germany*
[2]*Dark Cosmology Centre, Niels Bohr Institute, Copenhagen University, Juliane Maries Vej 30, 2100 Copenhagen O, Denmark*
[3]*European Southern Observatory, Alonso de Córdova 3107, Vitacura, Casilla 19001, Santiago 19, Chile*

24 January 2013

ABSTRACT

We analyze the redshift evolution of the mass-metallicity relation in a sample of 110 Damped Lyα absorbers spanning the redshift range $z = 0.11 - 5.06$ and find that the zero-point of the correlation changes significantly with redshift. The evolution is such that the zero-point is constant at the early phases of galaxy growth (i.e. no evolution) but then features a sharp break at $z = 2.6 \pm 0.2$ with a rapid incline towards lower redshifts such that damped absorbers of identical masses are more metal rich at later times than earlier. The slope of this mass metallicity correlation evolution is 0.35 ± 0.07 dex per unit redshift.

We compare this result to similar studies of the redshift evolution of emission selected galaxy samples and find a remarkable agreement with the slope of the evolution of galaxies of stellar mass $\log(M_*/M_\odot) \approx 8.5$. This allows us to form an observational tie between damped absorbers and galaxies seen in emission.

We use results from simulations to infer the virial mass of the dark matter halo of a typical DLA galaxy and find a ratio $(M_{vir}/M_*) \approx 30$.

We compare our results to those of several other studies that have reported strong transition-like events at redshifts around $z = 2.5 - 2.6$ and argue that all those observations can be understood as the consequence of a transition from a situation where galaxies were fed more unprocessed infalling gas than they could easily consume to one where they suddenly become infall starved and turn to mainly processing, or re-processing, of previously acquired gas.

Key words: galaxies: formation – galaxies: evolution – galaxies: high-redshift – galaxies: ISM – galaxies: mass-metallicity relation – quasars: absorption lines – cosmology: observations

1 INTRODUCTION

The conversion of gas into stars and the ensuing enrichment of the primordial gas with heavier elements is a fundamental process of cosmic evolution, its monotonic nature making it akin to an arrow of time for that evolution. Heavy elements are at high redshifts most easily detected in absorption and Damped Lyman α absorbers (DLAs, Wolfe et al. (1986)) allow us to trace the metallicity of the cold gas in galaxies back to redshifts of $z \gtrsim 5$ (e.g., Lu et al. 1996; Prochaska et al. 2003; Rafelski et al. 2012). Initially it was thought that DLA studies directly would provide us with the history of metal enrichment and that models based on DLA samples would be able to fully describe this evolution (e.g., Pei & Fall 1995; Cen & Ostriker 1999). However, the data displayed a surpris-

ingly weak dependence of the DLA metallicities on redshift (for a review see Pettini 2006). Also, the population of Lyman-break galaxies (LBGs) were discovered and some of these were found to have significantly higher metallicities than found in the DLA systems at similar redshifts (e.g., Pettini et al. 2002). The relation between DLAs and LBGs was subsequently the subject of several studies (Fynbo et al. 1999; Bunker et al. 1999; Warren et al. 2001; Møller et al. 2002; Weatherley et al. 2005; Rauch et al. 2008) and it was found that the difference between the two sets of galaxies can be understood from their very different selection functions (gas cross-section vs. UV luminosity selection). Also, it is becoming increasingly clear that correlations between metallicity and other fundamental galaxy parameters like luminosity, stellar mass, and star-formation rate are central to understanding the galaxy population both locally and at high redshifts (e.g., Tremonti et al. 2004; Savaglio et al. 2005; Calura et al. 2009; Mannucci et al. 2010).

⋆ E-mail: pmoller@eso.org

There is mounting evidence that DLA galaxies at $z > 2$ follow similar relations (Møller et al. 2004; Ledoux et al. 2006; Fynbo et al. 2008; Pontzen et al. 2008; Prochaska et al. 2008; Krogager et al. 2012).

The Lyman break technique and searches for DLAs in quasar spectra represent two widely different methods for finding galaxies at high redshifts and as argued above they are now understood to select different sub-samples of the high redshift galaxy population. Yet, there is an overlap between the two which can be exploited to gain a more detailed understanding of the galaxies in the overlapping region.

Searches for high redshift Lyα emitters is a third and independent method which again selects an independent well defined sub-sample of the underlying sample of all high redshift galaxies. Nilsson et al. (2009, 2011) found a remarkable property of Lyα emission selected galaxies namely an apparently sudden transition in their dust properties between redshifts 2.3 and 3 (confirmed by Ciardullo et al. 2012). In an unrelated study of highly reddened quasars Fynbo et al. (2013) reported a sudden drop in the detection rate of dusty quasar host galaxies at redshifts above 2.6 in good agreement with the transition of dust in Lyman α emitters at $z \simeq 2.5$.

In the same redshift range a transition in the mode of star formation is seen to take place in galaxy formation models (Oser et al. 2010) and Mannucci et al. (2010) reported that here a tight 3-way relation between mass, star formation and metallicity appears for the first time. This relation is thought to be caused by the interplay between infall of pristine gas and the outflow of enriched gas. The fact that it breaks down at $z \gtrsim 3$ suggests that the balance between inflow and outflow may be changing above and below this redshift, possibly caused by differences in the initial mass function (Bailin et al. 2010) or the thermodynamics of the intergalactic medium (Dixon & Furlanetto 2009).

Ledoux et al. (2006) showed that there is a strong mass metallicity relation for DLAs out to redshifts beyond $z = 4$ but they also reported tentative evidence that this relation was changing with redshift. The aim of this paper is to further investigate and quantify if there is indeed a redshift evolution of the DLA mass metallicity relation, how this relates to the redshift evolution of the mass metallicity relation of galaxies (Maiolino et al. 2008) and in particular how this is related to the phase transition in the physics of galaxies and star formation at a redshift around 2.5-2.6 as described above.

2   REDSHIFT EVOLUTION OF THE METALLICITY MASS RELATION

2.1   Sample definition

Our basis is the sample of 70 absorbers from Ledoux et al. (2006) (their Table 1). In order to increase the redshift coverage over that sample we have searched the literature for DLAs at both very low and very high redshifts with published spectroscopic observations of sufficiently high resolution. We found a total of 14 low redshift DLAs (in the redshift range 0.1 - 1.5, Table 1) and we include them all here. At high redshifts we selected the 22 DLAs observed with HIRES from Rafelski et al. (2012) which provides a homogeneous high redshift sample providing good coverage back to $z = 5.06$ (Table 2). In the sample we also included four newly observed objects from our X-shooter DLA survey (Fynbo et al. 2010) since the parameters required were already extracted and published (Table 3). Our total sample therefore includes 110 systems sampling
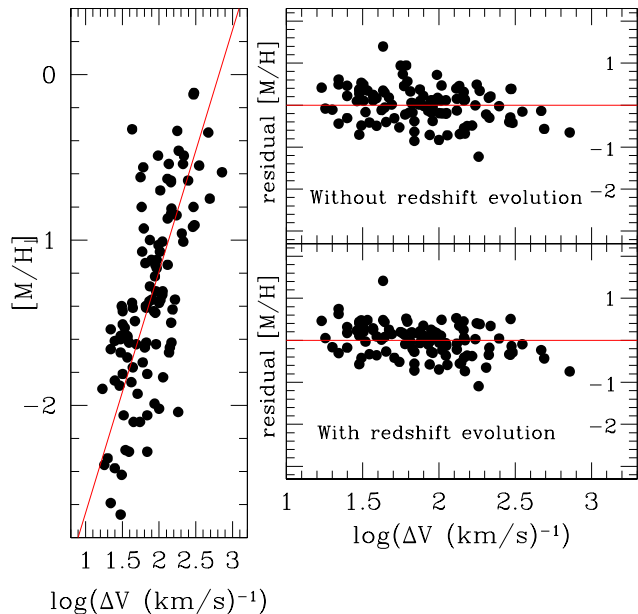

Figure 1. *Left frame:* Metallicity versus velocity width of each system in our sample. The best fit linear relation using a slope of 1.46 (see text) is drawn as a red line. *Right frames top to bottom:* Residuals after subtraction of the fit with no redshift evolution (eq(2)) and after subtraction of the fit including redshift evolution (eq(2 and 5)).

the redshift range $z = 0.11$ to 5.06. This represents an increase in sample size of 60% but more importantly it allows us to study the redshift evolution over a large fraction of the age of the universe.

2.2   Method

There is a relation between the velocity width of a DLA system and the gravitational mass of the host (Haehnelt et al. 1998; Pontzen et al. 2008) which makes it possible to use the velocity width, ΔV, as a proxy for the mass. In this paper we shall use the ΔV as defined in Ledoux et al. (2006) and for consistency we carefully choose suitable low ionization absorption lines as described in that work. To convert the published high resolution line profile data to electronic data we used the ADS Dexter data extraction applet which is a tool to extract data from figures from the ADS article service (Demleitner et al. 2001). The selected lines and the resulting ΔV are listed in Tables 1-2.

Ledoux et al. (2006) found the slope of the metallicity-ΔV relation to be 1.46 and no evidence was found for an evolution of this slope with redshift. We shall therefore at first conservatively adopt this slope. This forms our conservative assumption, but in order to certify that our conclusions do not depend on this assumption we shall also repeat the entire analysis with less conservative assumptions below.

The sample is plotted in the left panel of Fig. 1 where we also plot the best fit linear relation for a slope of 1.46. The errors on [M/H] are typically in the range $0.05 - 0.20$ and it is seen that the errors on the measurements are far too small to account for the scatter. As a first step we shall now determine the internal scatter of the distribution. To do this we assume that the measurement errors on the metallicity (σ_{met}) as well as the natural internal scatter of the relation (σ_{nat}) both follow normal distributions and that the two are statistically independent. This allows us to define a total predicted

Table 1. Metallicities and velocity widths of low-ionization lines for $z < 1.5$ DLAs (metallicity measurements are from various papers quoted in the table footnote)

Quasar	z_{abs}	$\log N(\mathrm{H\,I})$	[X/H]	X	ΔV (km s^{-1})	Selected transition lines [1]	Refs. [2]
B 0105−008	1.3710	21.70 ± 0.15	-1.40 ± 0.16	Zn	31	CrIIλ2056	a
J 0256+0110	0.725	20.70 ± 0.20	-0.11 ± 0.20	Zn	299	MgIλ2852	b
Q 0302−223	1.0094	20.36 ± 0.11	-0.56 ± 0.12	Zn	61	SiIIλ1808	c
Q 0449−1645	1.0072	20.98 ± 0.06	-0.96 ± 0.08	Zn	204	Al3λ1862	d
Q 0454+039	0.8597	20.69 ± 0.06	-1.01 ± 0.12	Zn	111	FeIIλ2260	c
Q 0933+733	1.479	21.62 ± 0.10	-1.58 ± 0.10	Zn	30	FeIIλ2249	e
Q 0948+433	1.233	21.62 ± 0.05	-1.14 ± 0.06	Zn	65	FeIIλ2260	e
J 1009+0713	0.1140	20.68 ± 0.10	-0.62 ± 0.16	S	56	TiIIλ3384	f
J 1107+0048	0.740	21.00 ± 0.04	-0.54 ± 0.16	Zn	212	MgIλ2852	b
Q 1354+258	1.4200	21.54 ± 0.06	-1.61 ± 0.16	Zn	25	FeIIλ2260	g
J 1431+3952	0.6018	21.2 ± 0.1	-0.80 ± 0.21	Zn	58	MnIIλ2576	a
J 1623+0718	1.3357	21.35 ± 0.10	-1.07 ± 0.13	Zn	59	FeIIλ2260	a
J 2328+0022	0.652	20.32 ± 0.06	-0.49 ± 0.16	Zn	97	MgIλ2852	b
B 2355−106	1.1723	21.0 ± 0.1	-0.87 ± 0.20	Zn	131	MgIλ2852	a

[1] Transition lines used to determine the velocity widths of low-ionization line profiles.
[2] References: [a] Ellison et al. (2012); [b] Péroux et al. (2006); [c] Pettini et al. (2000); [d] Péroux et al. (2008); [e] Rao et al. (2005); [f] Meiring et al. (2011); [g] Pettini et al. (1999).

Table 2. Metallicities and velocity widths of low-ionization lines for $z \sim 4$ DLAs (metallicity measurements are from Rafelski et al. (2012) based on element X with an upward correction of 0.3 dex for Fe)

Quasar	z_{abs}	$\log N(\mathrm{H\,I})$	[X/H]	X	ΔV (km s^{-1})	Selected transition lines [1]
J 0040−0915	4.7394	20.30 ± 0.15	-1.40 ± 0.17	Fe+0.3	67	FeIIλ1608
J 0747+4434	4.0196	20.95 ± 0.15	-2.28 ± 0.20	Fe+0.3	69	FeIIλ1608
J 0817+1351	4.2584	21.30 ± 0.15	-1.15 ± 0.15	S	89	SIIλ1250
J 0825+3544	3.2073	20.30 ± 0.10	-1.68 ± 0.16	Fe+0.3	30	FeIIλ1608
J 0825+3544	3.6567	21.25 ± 0.10	-1.83 ± 0.13	Si	89/138 [2]	SiIIλ1808/SiIIλ1304
J 1051+3107	4.1392	20.70 ± 0.20	-1.99 ± 0.21	S	87	SiIIλ1304
J 1051+3545	4.3498	20.45 ± 0.10	-1.88 ± 0.10	Si	29	SiIIλ1808
J 1051+3545	4.8206	20.35 ± 0.10	-2.28 ± 0.10	Si	39	SiIIλ1526
J 1100+1122	4.3947	21.74 ± 0.10	-1.68 ± 0.18	Fe+0.3	137	NiIIλ1709
J 1200+4015	3.2200	20.85 ± 0.10	-0.64 ± 0.10	S	145	NiIIλ1370
J 1200+4618	4.4765	20.50 ± 0.15	-1.38 ± 0.16	Fe+0.3	88/113 [2]	FeIIλ1611/SiIIλ1304
J 1201+2117	3.7975	21.35 ± 0.15	-0.75 ± 0.15	Si	490	SiIIλ1808
J 1201+2117	4.1578	20.60 ± 0.15	-2.38 ± 0.15	Si	25	SiIIλ1526
J 1202+3235	4.7955	21.10 ± 0.15	-2.36 ± 0.16	Fe+0.3	18	CII$^\star\lambda$1335
J 1202+3235	5.0647	20.30 ± 0.15	-2.66 ± 0.16	Si	30	OIλ1302
J 1304+1202	2.9131	20.55 ± 0.15	-1.65 ± 0.16	S	64	FeIIλ1608
J 1304+1202	2.9289	20.30 ± 0.15	-1.54 ± 0.16	S	22	FeIIλ1608
J 1353+5328	2.8349	20.80 ± 0.10	-1.38 ± 0.10	S	43	SIIλ1253
J 1438+4314	4.3990	20.89 ± 0.15	-1.31 ± 0.15	S	91	FeIIλ1608
J 1541+3153	2.4435	20.95 ± 0.10	-1.49 ± 0.11	Si	47	SiIIλ1808
J 1607+1604	4.4741	20.30 ± 0.15	-1.71 ± 0.15	Si	37	SiIIλ1304
J 1654+2227	4.0022	20.60 ± 0.15	-1.66 ± 0.16	Fe+0.3	22	FeIIλ1608

[1] Transition lines used to determine the velocity widths of low-ionization line profiles.
[2] For this system no line fulfilled the optimal criteria fully so we measured both a very weak line and a strong (slightly saturated) line. We list both lines and both measurements but we use the mean of the two.

σ

$$\sigma_{\mathrm{tot}}(i) = (\sigma_{\mathrm{met}}^2(i) + \sigma_{\mathrm{nat}}^2)^{1/2} \qquad (1)$$

for each observation, "i". For a given slope (α_0) and zero point (zp) of the metallicity-mass relation

$$[M/H] = \alpha_0 \log(\Delta V) + zp \qquad (2)$$

we can now assign a goodness of fit as the sum of the squares of the deviations of the fit to the data

$$C_{\mathrm{dof}}^2 = \sum_{i=1}^{110} (([M/H](i) - \alpha_0 \log(\Delta V(i)) - zp)/\sigma_{\mathrm{tot}}(i))^2)/dof \qquad (3)$$

where the degrees of freedom (dof) in this case is 108. C_{dof}^2 is equivalent to the χ^2 per degree of freedom of the distribution if

Table 3. DLA sample: average metallicities and velocity widths of low-ionisation line profiles [*]

Quasar	Other name	z_{em}	z_{abs}	$\log N(\text{H\,I})$	[X/H]	X	ΔV (km s^{-1})	Selected transition lines [1]	Refs. [2]
Q 0151+048		1.93	1.934	20.34 ± 0.02	-1.93 ± 0.04	Si	51	Si IIλ1304	a, b
Q 0918+1636	SDSS J 091826.16+163609.0	3.07	2.583	20.96 ± 0.05	-0.12 ± 0.05	Zn	295	Si IIλ1808	c
Q 0918+1636	SDSS J 091826.16+163609.0	3.07	2.412	21.26 ± 0.06	-0.55 ± 0.16	Zn	352	Si IIλ1808	d
Q 2222−0946		2.93	2.345	20.65 ± 0.05	-0.46 ± 0.07	Zn	185	Si IIλ1808	e

[1] Transition lines used to determine the velocity widths of low-ionization line profiles.
[2] References: [a] Zafar et al. (2011); [b] Ellison et al. (2012); [c] Fynbo et al. (2011); [d] Thorsen (2011); [e] Fynbo et al. (2010).

σ_{nat} is correctly chosen. We can therefore use eq(3) to select all pairs of (zp, σ_{nat}) for which $C^2_{dof} = 1$, and we then choose the pair for which σ_{nat} has its minimum value as the globally best fit: $(\alpha_0, zp, \sigma_{nat}) = (1.46, -4.111, 0.4181)$. In the top right panel of Fig. 1 we plot the residuals after subtraction of this fit.

2.3 Redshift evolution

By splitting their sample into a high and a low redshift sample, Ledoux et al. (2006) already pointed out that while the slope of the correlation did not appear to change, there was a shift of the correlation. Here we seek a more general formulation of this redshift evolution.

Inverting eq(2) we can interpret each absorber of the sample as an independent measurement of the zero point

$$zp(i) = [M/H](i) - \alpha_0 \log(\Delta V(i)) \quad (4)$$

with an uncertainty of $\sigma_{tot}(i)$. This allows us to check if we see an evolution of zp as a function of redshift. The function describes directly the evolution (shift) of the mass-metallicity relation at a given intercept (mass) and we have chosen to normalize the zero point to a mass of 100 km/s, which is a typical mass in our sample, and to name it $[M/H]_{100\ km/s}(z)$. This function represents the mean metallicity of a galaxy with a mass of 100 km/s as a function of redshift.

In Fig. 2 we show $[M/H]_{100\ km/s}(z)$ plotted versus redshift, i.e. we plot the evolution of the mean metallicity of the cold gas in a galaxy of a mass of 100 km/s from redshift 5 to 0. The horizontal bars in Fig. 2 show the z range of each bin, while the vertical bars show the propagated uncertainty of the $[M/H]_{100\ km/s}(z)$.

From Fig. 2 we see clear evidence for a steady and continuous incline of $[M/H]_{100\ km/s}(z)$ from redshift 2.6 to 0. An incline of $M(z)$ means that the metallicity-mass relation changes such that for any given mass the galaxy becomes more metal rich at later times. At earlier times than redshift 2.6 there is no evidence for any evolution and it appears that the mass-metallicity relation was constant from $z = 5$ to $z = 2.6$.

We will take this apparent "two phase" nature of the early universe as our working hypothesis and proceed to fit the evolution with a constant at high redshifts and the late incline with a linear function. The transition between the two then happens at the transition redshift z_{tran} and we get

$$zp(z) = \begin{cases} \beta_{early}\,(const) & \text{for } z > z_{tran}, \\ \alpha_{late}\,z + \beta_{late} & \text{for } z \leqslant z_{tran} \end{cases} \quad (5)$$

where the constant value at high redshift is defined by the requirement that $zp(z)$ is continuous at z_{tran}, i.e. β_{early} is not a free parameter.
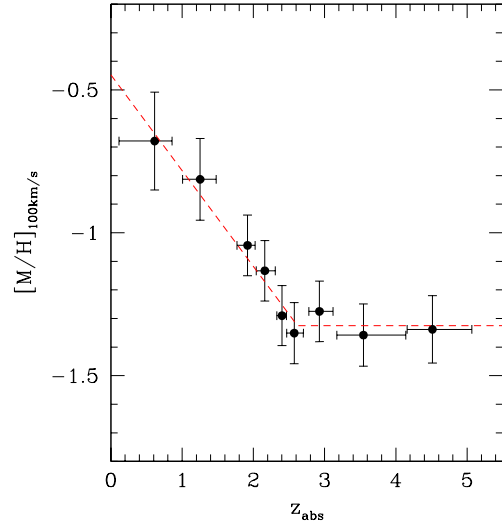

Figure 2. Redshift evolution of the zero point of the DLA mass-metallicity relation. We have normalized the function to a gravitational well mass of 100 km/s. The red line is a best fit to the data of the form given in eq(5). There is no evidence for evolution before redshift 2.6, and then a sharp break at $z = 2.6$ with an onset of strong evolution. The evolution is such that the metallicity of a galaxy of a given mass grows by 0.35 ± 0.07 dex per unit redshift. The fit was computed as a fit to all 110 data points, not to the binned data.

Table 4. Fitted evolution parameters for $\alpha_0 = 1.46$. The parameters are defined in eq(5).

α_{late}	-0.35 ± 0.07
β_{late}	-3.33 ± 0.16
z_{tran}	2.62 ± 0.20
β_{early}	-4.25 ± 0.05

We do not fit the binned data in Fig. 2, rather we proceed using the method described in Sect. 2.2 fitting simultaneously the parameters in eq(2) and eq(5) for all 110 systems. In this way we find z_{tran}=2.618 and σ_{nat}=0.3759 for α_0=1.46 and 106 dof. In Table 4 we provide all the parameters for the fit and in Fig. 2 this best fit is shown as red dashed lines. In Fig. 1 (lower panel to the right) we plot the residuals ($res_{[M/H]}$) after subtraction of this fit. Comparing the upper and lower right frame it is easy to notice the decreased scatter of the residuals (from 0.4181 to 0.3759).
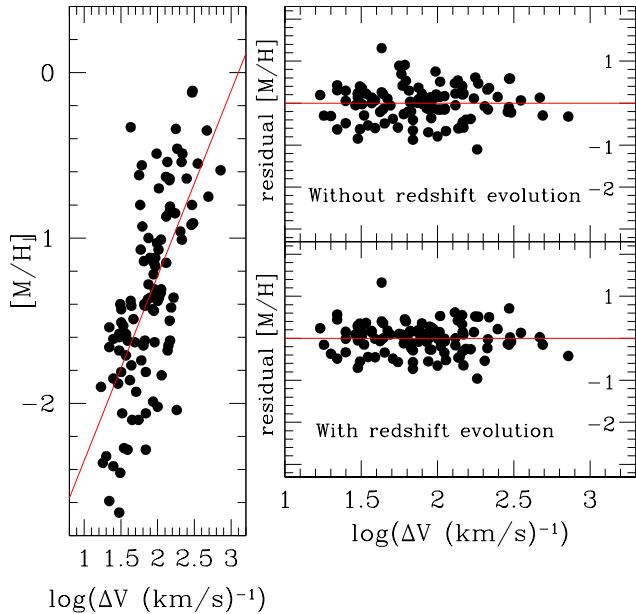
Figure 3. Same as Fig. 1 except that we here fit for the slope and find a best fit for $\alpha_0 = 1.12$.

Figure 4. Here we plot the redshift evolution of the galaxy mass-metallicity relations from Maiolino et al. (2008) for different stellar masses (full curves) and the DLA data points and fit (dashed line) from Fig. 2. There is a remarkable agreement between the slope of the redshift evolution of the DLA galaxies and that of low-mass galaxies from Maiolino's study.

2.4 Testing the importance of the assumed α_0

In the above analysis we started by fixing the slope of the mass metallicity relation to α_0=1.46 as found by Ledoux et al. (2006) who used a bisector fit. We agree that because of the large scatter the bisector is the best way of determining the slope, but we wish to test if another assumption would significantly change our result regarding the redshift evolution. We therefore now relax this constraint and repeat the analysis treating α_0 as a free parameter with an additional minimization fit. We find that the best fit in the form of eq(2) is obtained with a slope of $\alpha_0 = 1.12$ as shown in Fig. 3. The resulting fit to the redshift evolution is however almost unchanged. The transition redshift is now found at z_{tran}=2.622 (a change of only 0.003) and the redshift evolution slope is 0.37 dex per unit redshift (a change of 0.02). Both values are well within the 1σ errors of the original fit.

We conclude from this that the specific assumption of the slope of the underlying mass metallicity relation has almost no effect on the results regarding the redshift evolution of the relation and that the result displayed in Fig. 2 is very robust. In hindsight we can now understand the riddle which for almost 2 decades was perplexing cosmologists: "Why do we not see clear evidence for cosmic chemical evolution in high redshift DLAs?" (e.g., Pettini et al. 1994).

2.5 Comparison with the redshift evolution of the galaxy stellar mass-metallicity relation

Maiolino et al. (2008) provided galaxy mass-metallicity relations back to a redshift of 3.5 as a function of galaxy stellar mass (their eq. 2). We have computed a grid of those relations and overplot them on our DLA measurements in Fig. 4. It can be seen that Maiolino et al. (2008) produces relations of metallicity as a function of redshift of increasing slopes with decreasing stellar masses. In the mass range $\log(M_*/M_\odot) = 8.5 - 9.0$, it is apparent that the slope matches the evolution of DLAs below $z \approx 2.6$ almost
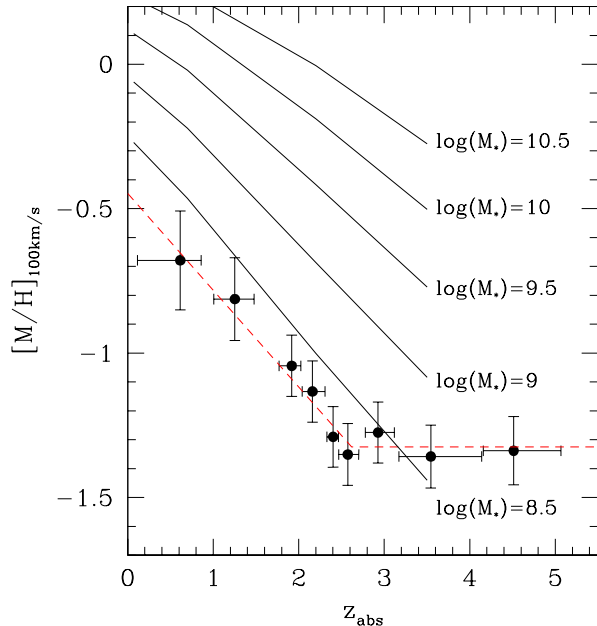
perfectly. The fact that the evolution of the zero point of the DLA velocity-metallicity correlation with redshift matches the galaxy stellar mass-metallicity evolution so well strongly supports the idea that we are witnessing in the DLA data a mass-metallicity relation akin to galaxies as initially suggested by Ledoux et al. (2006) further.

It is still a matter of debate how exactly emission-line based metallicities relate to the metallicity of the absorbing gas. It is usually thought that the DLA gas can have lower metallicities than those determined from emission line fluxes (e.g. Péroux et al. 2012). However, there are uncertainties in the recipes used to measure oxygen abundances from emission lines (e.g., Kudritzki et al. 2012) and in the choice of a suitable element to derive absorption-line metallicities. Other works have indeed found consistency between the two measurements (e.g., Bowen et al. 2005; Krogager 2013). Here, we conservatively assume that the DLA gas either has the same metallicity or a metallicity up to 0.5 dex lower than that derived from emission lines. Any effects related to α-element over-abundance will also be covered by this assumption. Given the remarkable similarity of the slopes of the relations shown in Fig. 4, we then estimate that the "typical" DLA in our sample exhibiting $\Delta V = 100$ km s^{-1} has a stellar mass $\log(M_*/M_\odot)$ of the order of 8.5. This is in agreement with the early result that due to the effect of gas cross-section selection even the most massive DLA galaxies only correspond to the least massive Lyman-Break galaxies (Fynbo et al. 1999). As a matter of fact, there is only a small range of overlapping metallicity between our DLA sample and the galaxy sample in the study of Maiolino et al. (2008).

In order to generalize the comparison, we then determined the best fit to a range of models in the very lowest range of masses covered by Maiolino's data, which constitutes the small overlap region with the DLA galaxies. In practice we created a finer grid of the Maiolino models than shown in Fig. 4, we then slid our data points
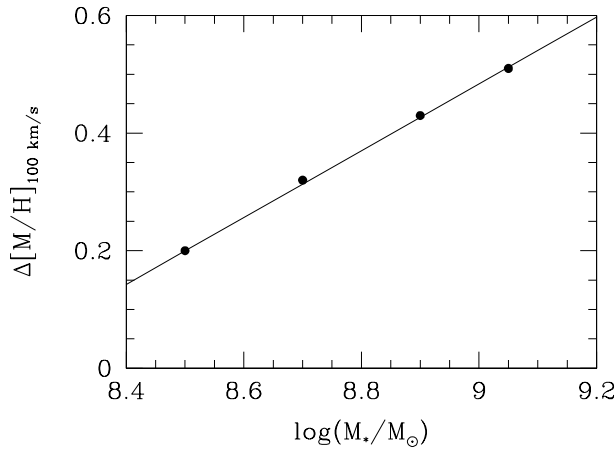
Figure 5. Offsets (Δ[M/H]$_{100\mathrm{km/s}}$) required to fit the data points in Fig. 4 to a grid of stellar masses using the Maiolino models in the region of overlap. The offsets are well fitted by a linear relation with slope 1.76^{-1}.

in Fig. 4 up to match each model defined by a given stellar mass and determined the offset (Δ[M/H]$_{100\mathrm{km/s}}$) required. The offsets are shown in Fig. 5 as a function of stellar mass and it is seen that in the mass range considered the offsets are well fitted by a linear relation with slope 1.76^{-1}.

The correction in metallicity when comparing absorption to emission is not yet well known so we allow for this as a free parameter, $C_{[M/H]}$, which must be added to the absorption-line metallicity to make it consistent with the emission-line metallicity. Finally, in the redshift range considered we found an evolution with redshift such that Δ[M/H]$= -0.35\Delta z$ for a given mass. We can now write up the relation:

$$\log(M_*/M_\odot) = 1.76([M/H] + C_{[M/H]} + 0.35z + 5.04) \quad (6)$$

between DLA metallicity and stellar mass of the DLA host galaxy. Here 1.76 on the right side comes from the slope of the relation in Fig. 5, $0.35z$ from the redshift evolution (α_{late} in eq(5)) and 5.04 is the empirically determined zero point of the relation.

A number of important caveats should be noted before using this relation.

• There is a large scatter in this relation (0.38 dex in $[M/H]$) so it is only useful as a statistical tool on large samples. Application to single systems will probably not be meaningful.
• The relation is found from, and only known to be correct in, the small range of overlap between the two samples.
• The relation is formally valid back to $z = 2.6$ and the fit is excellent between $z = 2.6$ and $z = 0$. At higher redshifts, flux-limited galaxy studies only sample the most massive galaxies, while the DLA systems sample halos of roughly the same mass at all redshifts. There is therefore a huge gap between the two samples at high redshifts and we have not tried to extract a similar relation past the break at $z = 2.62$. The results provided in this paper suggest that the relation remains constant at higher redshifts (i.e., z should be replaced by 2.62 in Eq. 6), but this has not yet been verified by high-redshift galaxy studies.

2.6   Virial masses

We now ask the question what the virial mass (M_{vir}) of the dark matter halo of a typical DLA galaxy is. Via identification of DLAs in dark matter halos of their cosmological simulations,

Pontzen et al. (2008) were able to confirm that the relation between ΔV and metallicity reported by Ledoux et al. (2006) is indeed a mass-metallicity relation. A relation between ΔV and virial mass of the DM halo is clearly seen in their simulations but the relation has a significant scatter. They also tend to underestimate the velocity widths of absorption-line profiles (their fig. 8). Taking this into account, a typical DLA with width 100 km s^{-1} would correspond to a virial mass $\log(M_{\mathrm{vir}}/M_\odot)$ of the order of 10. This leads to a mass-to-light ratio of ~ 30 for a typical DLA galaxy at redshifts below $z \approx 2.6$. We note that significantly larger virial masses have been inferred for DLA host halos from clustering arguments (Font-Ribera et al. 2012).

3   DISCUSSION AND CONCLUSIONS

3.1   Transition redshift of the mass metallicity relation

We confirm the reported mass metallicity relation for high redshift DLAs and we confirm that there is indeed a redshift evolution of this relation (Møller et al. 2004; Ledoux et al. 2006; Pontzen et al. 2008) but only in the later phase of cosmic evolution. At high redshifts the mass metallicity relation is constant while there is a break at $z = 2.6 \pm 0.2$ with a sudden onset of redshift evolution with a slope of 0.35 ± 0.07 dex per unit redshift.

Previously similar sharp transitions in the properties of Lyα emitters identified as ULIRGs and QSOs (Nilsson & Møller 2009; Bongiovanni et al. 2010; Nilsson & Møller 2011) and in the detection rate of highly reddened quasar host galaxies (Fynbo et al. 2013) at redshifts around $z = 2.5 - 2.6$ have been reported. The close coincidence of the redshifts of those transitions, which also precisely coincides with the peak of the star formation rate density (Hopkins & Beacom 2006) makes it plausible that they must all be related in some way. Lyα emitters only form a sub-set of the population of high redshift galaxies. DLAs however trace the gas both in Lyα emitting galaxies (e.g. Møller & Warren (1993)) and in galaxies with no Lyα emission (e.g. Fynbo et al. (2011); Bouché et al. (2012)) and in fact most DLA galaxies are non-detected in Lyα (Møller et al. 2004). It is therefore now evident that the transition seen for Lyα emitters is not an artefact of the Lyα emission selection method. A recent detailed study of the mass metallicity relation of galaxies seen in emission Mannucci et al. (2010) showed that the relation in fact forms a plane with the star formation rate as the third parameter. Their description forms a perfect fit in the redshift range $z = 0 - 2.5$, but breaks completely down at z=3 as seen in their Figure 4, right panel.

3.2   Slope of the redshift evolution

The redshift evolution below $z = 2.6$ is such that for a given virial halo mass the gas has higher metallicity at lower redshifts than at higher redshifts. This is in agreement with results for galaxies reported by Savaglio et al. (2005) and Maiolino et al. (2008). We find the slope of the evolution to be 0.35 ± 0.07 dex per unit redshift in agreement with the slope found in the low stellar mass range for similar studies of galaxies.

3.3   The stellar masses of DLAs

Identifying the galaxies that harbour the DLAs at high redshifts has been a holy grail for DLA studies ever since the first DLA was discovered. Attempts to do this on a case by case basis have been

mostly unsuccessful (e.g., Smith et al. 1989) and still only a couple of handful detections have been reported (Krogager et al. 2012). In this paper we were able to tie a direct link between a flux selected galaxy sample and our DLA sample using the evolution of the mass-metallicity relation to link them, and to provide an expression for the stellar mass of DLAs as a function of their metallicity and redshift.

3.4 A plausible cause of the transition: Infall starvation

The conclusions from a study of the redshift evolution of Lyα emitters (Nilsson et al. 2009) were that at redshifts above ~ 3 the objects were all star forming, with little or no dust, and with young blue populations, while at redshifts lower than ~ 2.5 a significant fraction of red, dusty, mixed population objects, even ULIRGs, were found. The simplest way to explain those observations as well as the new results reported here is a scenario in which primordial, or near-primordial, gas is constantly accreted onto the galaxies at high redshifts (Barkana & Loeb 2003; Weidinger et al. 2005; Dekel et al. 2009). If the amount of gas available for infall is larger than a galaxy can accept and process then they will all accrete at maximum capacity. As the gas is converted into stars and enriches the galaxy with metals, this sets up an unchanging universal relation between the mass and the metallicity of a galaxy. With respect to this relation one might refer to this early phase as a steady state of galaxy evolution.

In order to change the universal mass-metallicity relation, some other parameter has to change first and the only available parameter is the infall rate. We therefore propose that the trigger to start the evolution of the mass-metallicity relation is a drop in the infall rate of primordial gas at $z_{\mathrm{tran}} = 2.6$ below the point of balance for the steady state to be maintained.

This can be accomplished in two ways. Either the supply of metal poor gas simply drops far below that of metal enriched gas, or at the peak of the star formation rate at $z \simeq 2.6$ (Hopkins & Beacom 2006) powerful galactic winds create highly ionized halos which render it difficult for the infall to continue at the same high level. This effect is known as accretion quenching and was used by Bouché et al. (2010) who found that it was a necessary ingredient in their model in order to reproduce the observed star formation rate-mass and Tully-Fisher relations. The primary mode of galaxy stellar mass growth then shifts from gas accretion to merging. There is some theoretical evidence for this. Oser et al. (2010) reported that their simulations showed that there is a transition between redshifts of 3 and 2 where the galaxy growth changes from "in situ" formation of stars from accreted cold gas towards accretion of stars which were formed in satellites earlier. The new results we have presented here are observational support for this model as well as for the accretion efficiency controlled model by Bouché et al. (2010). There are similar obvious links to the sudden change in Lyα emission line selected samples at $z_{\mathrm{tran}} = 2.52$ and to the setup of the tight 3-way relation between mass, star formation and metallicity (FMR) between $z = 3.3$ and 2.5. (Mannucci et al. 2010). In the latter work it was found that infall rates must have been $\simeq 10^3$ times higher at $z = 3.3$ than locally.

3.5 Future work and outlook

The dominating source of errors is the internal scatter, not the measurement errors. Using a larger sample or a sample with smaller errors will therefore not improve the results much. The best way to obtain a significant improvement is to identify and understand the source of the scatter.

N-body simulations of the galaxy growth via "in situ" formation of stars versus accretion of satellites including gas metallicity predictions would be an important tool to test if the proposed model is correct.

In order to be able to test if the break at $z = 2.6$ is also present in galaxy emission selected samples those would need to reach much lower stellar mass at redshifts between 4 and 5 to make it possible to tie them together with DLA samples. This will likely not be possible until E-ELT class telescopes become available.

REFERENCES

Bailin, J., Stinson, G., Couchman, H., Harris, W. E., Wadsley, J., & Shen, S., 2010, ApJ, 715, 194

Barkana, R. & Loeb, A., 2003, Nature, 421, 341

Bongiovanni, A., Oteo, I., Cepa, J., et al., 2010, A&A, 519, L4

Bouché, N., Dekel, A., Genzel, R., et al., 2010, ApJ, 718, 1001

Bouché, N., Murphy, M. T., Péroux, C., et al., 2012, MNRAS, 419, 2

Bowen, D. V., Jenkins, E. B., Pettini, M., & Tripp, T. M., 2005, ApJ, 635, 880

Bunker, A. J., Warren, S. J., Clements, D. L., Williger, G. M., & Hewett, P. C., 1999, MNRAS, 309, 875

Calura, F., Pipino, A., Chiappini, C., Matteucci, F., & Maiolino, R., 2009, A&A, 504, 373

Cen, R. & Ostriker, J. P., 1999, ApJ, 519, L109

Ciardullo, R., Gronwall, C., Wolf, C., et al., 2012, ApJ, 744, 110

Dekel, A., Birnboim, Y., Engel, G., et al., 2009, Nature, 457, 451

Demleitner, M., Accomazzi, A., Eichhorn, G., Grant, C. S., Kurtz, M. J., & Murray, S. S., 2001, Astronomical Society of the Pacific Conference Series, 238, 321

Dixon, K. L. & Furlanetto, S. R., 2009, ApJ, 706, 970

Ellison, S. L., Kanekar, N., Prochaska, J. X., Momjian, E., & Worseck, G., 2012, MNRAS, 424, 293

Font-Ribera, A., Miralda-Escudé, J., Arnau, E., et al., 2012, ArXiv e-prints

Fynbo, J. P. U., Krogager, J.-K., Venemans, B., Noterdaeme, P., Vestergaard, M., Møller, P., Ledoux, C., & Geier, S., 2013, ApJS, 204, 6

Fynbo, J. P. U., Laursen, P., Ledoux, C., et al., 2010, MNRAS, 408, 2128

Fynbo, J. P. U., Ledoux, C., Noterdaeme, P., et al., 2011, MNRAS, 413, 2481

Fynbo, J. P. U., Prochaska, J. X., Sommer-Larsen, J., Dessauges-Zavadsky, M., & Møller, P., 2008, ApJ, 683, 321

Fynbo, J. U., Møller, P., & Warren, S. J., 1999, MNRAS, 305, 849

Haehnelt, M. G., Steinmetz, M., & Rauch, M., 1998, ApJ, 495, 647

Hopkins, A. M. & Beacom, J. F., 2006, ApJ, 651, 142

Krogager, J.-K., 2013, MNRAS, in prep.

Krogager, J.-K., Fynbo, J. P. U., Møller, P., Ledoux, C., Noterdaeme, P., Christensen, L., Milvang-Jensen, B., & Sparre, M., 2012, MNRAS, 424, L1

Kudritzki, R.-P., Urbaneja, M. A., Gazak, Z., Bresolin, F., Przybilla, N., Gieren, W., & Pietrzyński, G., 2012, ApJ, 747, 15

Ledoux, C., Petitjean, P., Fynbo, J. P. U., Møller, P., & Srianand, R., 2006, A&A, 457, 71

Lu, L., Sargent, W. L. W., Barlow, T. A., Churchill, C. W., & Vogt, S. S., 1996, ApJS, 107, 475

Maiolino, R., Nagao, T., Grazian, A., et al., 2008, A&A, 488, 463

Mannucci, F., Cresci, G., Maiolino, R., Marconi, A., & Gnerucci, A., 2010, MNRAS, 408, 2115

Meiring, J. D., Tripp, T. M., Prochaska, J. X., et al., 2011, ApJ, 732, 35

Møller, P., Fynbo, J. P. U., & Fall, S. M., 2004, A&A, 422, L33

Møller, P. & Warren, S. J., 1993, A&A, 270, 43

Møller, P., Warren, S. J., Fall, S. M., Fynbo, J. U., & Jakobsen, P., 2002, ApJ, 574, 51

Nilsson, K. K. & Møller, P., 2009, A&A, 508, L21

—, 2011, A&A, 527, L7

Nilsson, K. K., Östlin, G., Møller, P., Möller-Nilsson, O., Tapken, C., Freudling, W., & Fynbo, J. P. U., 2011, A&A, 529, A9

Nilsson, K. K., Tapken, C., Møller, P., Freudling, W., Fynbo, J. P. U., Meisenheimer, K., Laursen, P., & Östlin, G., 2009, A&A, 498, 13

Oser, L., Ostriker, J. P., Naab, T., Johansson, P. H., & Burkert, A., 2010, ApJ, 725, 2312

Pei, Y. C. & Fall, S. M., 1995, ApJ, 454, 69

Péroux, C., Bouché, N., Kulkarni, V. P., York, D. G., & Vladilo, G., 2012, MNRAS, 419, 3060

Péroux, C., Meiring, J. D., Kulkarni, V. P., Ferlet, R., Khare, P., Lauroesch, J. T., Vladilo, G., & York, D. G., 2006, MNRAS, 372, 369

Péroux, C., Meiring, J. D., Kulkarni, V. P., Khare, P., Lauroesch, J. T., Vladilo, G., & York, D. G., 2008, MNRAS, 386, 2209

Pettini, M., 2006, in The Fabulous Destiny of Galaxies: Bridging Past and Present, Le Brun, V., Mazure, A., Arnouts, S., & Burgarella, D., eds., p. 319

Pettini, M., Ellison, S. L., Steidel, C. C., & Bowen, D. V., 1999, ApJ, 510, 576

Pettini, M., Ellison, S. L., Steidel, C. C., Shapley, A. E., & Bowen, D. V., 2000, ApJ, 532, 65

Pettini, M., Rix, S. A., Steidel, C. C., Adelberger, K. L., Hunt, M. P., & Shapley, A. E., 2002, ApJ, 569, 742

Pettini, M., Smith, L. J., Hunstead, R. W., & King, D. L., 1994, ApJ, 426, 79

Pontzen, A., Governato, F., Pettini, M., et al., 2008, MNRAS, 390, 1349

Prochaska, J. X., Chen, H.-W., Wolfe, A. M., Dessauges-Zavadsky, M., & Bloom, J. S., 2008, ApJ, 672, 59

Prochaska, J. X., Gawiser, E., Wolfe, A. M., Castro, S., & Djorgovski, S. G., 2003, ApJ, 595, L9

Rafelski, M., Wolfe, A. M., Prochaska, J. X., Neeleman, M., & Mendez, A. J., 2012, ApJ, 755, 89

Rao, S. M., Prochaska, J. X., Howk, J. C., & Wolfe, A. M., 2005, AJ, 129, 9

Rauch, M., Haehnelt, M., Bunker, A., et al., 2008, ApJ, 681, 856

Savaglio, S., Glazebrook, K., Le Borgne, D., et al., 2005, ApJ, 635, 260

Smith, H. E., Cohen, R. D., Burns, J. E., Moore, D. J., & Uchida, B. A., 1989, ApJ, 347, 87

Thorsen, T. J., 2011, Master's thesis, Niels Bohr Institute, Copenhagen University, Juliane Maries Vej 30, DK-2100 Copenhagen O, Denmark

Tremonti, C. A., Heckman, T. M., Kauffmann, G., et al., 2004, ApJ, 613, 898

Warren, S. J., Møller, P., Fall, S. M., & Jakobsen, P., 2001, MNRAS, 326, 759

Weatherley, S. J., Warren, S. J., Møller, P., Fall, S. M., Fynbo, J. U., & Croom, S. M., 2005, MNRAS, 358, 985

Weidinger, M., Møller, P., Fynbo, J. P. U., & Thomsen, B., 2005, A&A, 436, 825

Wolfe, A. M., Turnshek, D. A., Smith, H. E., & Cohen, R. D., 1986, ApJS, 61, 249

Zafar, T., Møller, P., Ledoux, C., et al., 2011, A&A, 532, A51